

Energy Spectra and Elemental Composition Determination on Mountain Altitudes and Sea Level

A. Chilingarian^a, S. Ter-Antonyan^a, A. Vardanyan^a and
M. Roth^b, H.J. Gils^b, J. Knapp^b, H. Rebel^b and KASCADE Collaboration

^aCosmic Ray Division, Yerevan Physics Institute, Yerevan 36, Armenia

^bForschungszentrum und Universität Karlsruhe, Institut für Kernphysik, D-76021 Karlsruhe, Germany

The accurate measurement of the elemental composition and energy spectra of primary cosmic rays in the energy range $10^{14} - 10^{17}$ eV is vitally important. The information carried by Extensive Air showers (EAS) in this energy range is limited by significant fluctuations of the shower development, insufficient experimental sampling and uncertainties of the detector response. Additional uncertainties arise from different simulation procedures and statistical methods used for inferring results from the measurements. We propose to combine an advanced EAS simulation program like CORSIKA with the ANI multivariate statistical analysis package for an event-by-event analysis and for a standardization of the inference from EAS data. As an example, the possibilities of modern EAS installations at mountain altitudes and sea level are explored. The accuracies of the elemental composition determination based on measured components of EAS are presented. The Neural Networks classification and Bayesian Decision Making approaches are used and compared. The new nonparametric methods of primary energy estimations are discussed.

1. Introduction

The main objectives of EAS observations are the possible sources of cosmic rays and the mechanisms of particle acceleration in the interstellar medium. The particular physical quantities to be measured are the energy spectra and elemental composition of cosmic radiation incident on the Earth's atmosphere. The direct cosmic ray measurements on board of satellites and balloons are well described by the supernovae diffusive shock acceleration mechanism [1]. However, for energies above 10^{14} eV Fermi acceleration becomes less effective [2] and the most well-known peculiarity of cosmic rays - the so-called all particles spectrum knee - is detected in the region of $3 \times 10^{15} - 5 \times 10^{15}$ eV [3]. Several hypotheses are proposed for the explanation of the particle acceleration for such energies [4,5], but lack of precise and reliable results on the elemental composition around the "knee" prevents the strict physical inference of the new acceleration mechanism and possible so far known new types of natural high energy particle accelerators.

Theore, the problem of cosmic rays origin can only be solved if one succeeds in measuring the elemental composition of cosmic rays in the energy range of $10^{14} - 10^{17}$ eV. However, direct measurements in the mentioned energy region are impossible due to the small fluxes. Indirect methods based on registration of EAS have to be employed.

2. Interpretation of EAS data

When interpreting the results of ground-based experiments with cosmic rays serious ambiguities and contradictions often arise. These are connected with the nature of such indirect experiments which detect only secondary particles of late generations in the shower development. The characteristic quantities of the primary cosmic particle - its elemental species and energy - can be inferred from the experimental data only by the help of Monte Carlo (MC) simulations and specific classification algorithms. The significant lack in our knowledge about details of nucleus-nucleus interactions beyond (man made) accelerator energies

and the strong fluctuations of all shower parameters are the main problems in such analyses. However, it is very helpful to measure as many as possible independent parameters in each individual event in order to reduce uncertainties by correlations between observables. Thereby, more reliable information can be yielded to reconstruct the primary particle type and its energetic characteristics as well as the peculiarities of strong interactions at the top of the atmosphere.

In previously used methods, only the distributions (histograms) summarized over experiment and simulation, respectively, are compared and integral hypotheses, asking to what extent the data are compatible with a particular hypothesis about composition and scaling violation e.g. are tested. Thereby mostly qualitative conclusions were obtained. In contrast, the techniques proposed here provide the possibility to analyze EAS data on event-by-event basis [6].

We develop a unified theory of statistical inference, based on nonparametric models, in which various nonparametric approaches (density estimation, Bayesian decision making, error rate estimation, feature extraction, sample control during handling, neural net models, etc...) are implemented [7,8].

3. Bayesian and Neural Decision rules

In the present approach each event represents a point in the multidimensional space of the EAS parameters. The data are obtained with the ANI [9] and the KASCADE [10] detector installations using results of the air shower simulation code CORSIKA [11] and the ANI statistical analysis package [12].

In the Bayesian approach classifying a mixture of distributions losses due to incorrect classification [13] are minimized. Therefore the Bayesian decision rule takes the form (a simple loss function is assumed):

$$A = \max_i \{ \hat{p}(A_i/\mathbf{v}) \}, \quad i = 1, \dots, K \quad (1)$$

where the space of possible states of nature $\mathbf{A} \equiv (p, \alpha, O, Si, Fe)$ consists of $K=5$ groups of primary nuclei, \mathbf{v} is the multivariate measurement and $\hat{p}(A_i/\mathbf{v})$ are nonparametric estimates of

à posteriori densities, connected with conditional ones by the Bayes theorem:

$$\hat{p}(A_i/\mathbf{v}) = \frac{P_i \cdot \hat{p}(\mathbf{v}_i/A_i)}{p(\mathbf{v})} \quad (2)$$

Conditional densities are estimated by training samples (TS) obtained from CORSIKA simulation using Parzen's method with automatic kernel width adaptation. In this method some probability density values are calculated which correspond to different values of method parameters. Then the sequence obtained is ordered and the median of this sequence is chosen as final estimate. The probability density is estimated by:

$$\hat{p}(\mathbf{v}/A_i) = \frac{1}{2\pi^{d/2}h^d} \sum_j^{M_i} e^{-r_j^2/h^d} W_j, \quad i = 1, \dots, K \quad (3)$$

where d is the feature space dimensionality, M_i is the number of events in the i -th TS class, r_j is the distance to the j -th neighbor in the Mahalanobis metric

$$r_j = (\mathbf{v} - \mathbf{u}_j)^T R^{-1}(\mathbf{v} - \mathbf{u}_j). \quad (4)$$

R is a sampling covariance matrix of the class to which \mathbf{u} belongs, W_j are the event weights and h is the width of the kernel.

The Neural decision making is another nonparametric technique mapping the multidimensional measurements into one dimensional 'decision' (0-1) interval [14,15]. The "target" output $OUT^{target}(k)$ for events of the k -th category (we restrict ourselves to networks with a single output node) is determined to maximize the shift of the alternative classes from each other:

$$OUT^{target}(k) = \frac{k-1}{K-1}, \quad k = 1, \dots, K \quad (5)$$

$$OUT^{target}(k) \in (0, 1)$$

The actual event classification is performed by comparing the obtained output value with the predefined intervals in the (0, 1) interval. As expected the data flow passing through the trained net is divided into 5 clusters concentrated in the different regions of the (0, 1) interval (see figure 1).

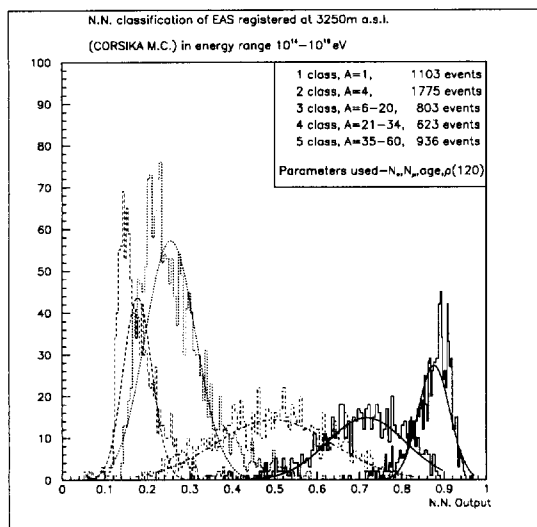


Figure 1. Neural network output results (histogram) compared to input densities (smooth curves)

This neural decision rule is also a Bayesian one, therefore the output signal of a properly trained feed-forward neural net is an estimate of the à posteriori probability density [16].

The expected minimal classification errors caused by the overlap of the distributions (the Bayes error) depend on the discriminative power of the feature subset selected and on the learning power. By moving the decision points along the $(0, 1)$ interval we can change the relation between the errors of the first and second kind (the position of the decision points is the neural analog of the loss function in the Bayesian approach).

The primary nucleus estimation was done for the ANI experiment operating on Aragats mountain research station of the Yerevan Physics Institute, Armenia. The experimental complex consists of a ground-based shower array, muon detectors installed in a underground hall and a high resolution electron density detector. The location of the station (3250 m above sea level) permits the accurate determination of the energy of the primary particle, and provides also an estimation

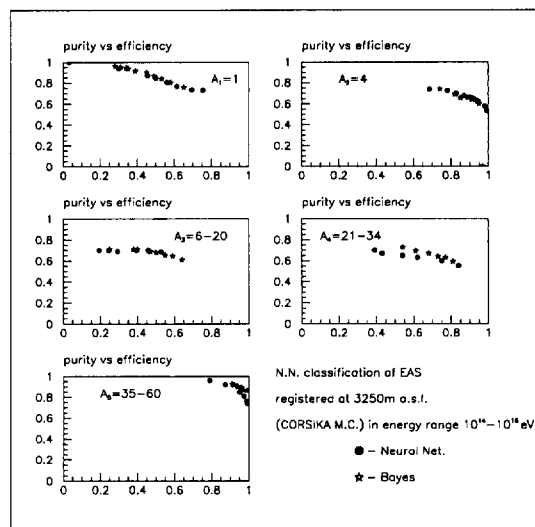


Figure 2. Purity vs efficiency for Neural Net and Bayes classification methods

of the primary particle type with rather good accuracy.

The purity-efficiency plots (figure 2) show the good agreement of both nonparametric approaches. Different points were obtained by altering the à priori probabilities in the Bayesian method and the decision points in the neural method, respectively.

4. Variable Selection and Energy Estimation

Figure 3 indicates that one-dimensional distributions of simulated EAS parameters (numbers of electrons and muons, age and electron density at a distance of 120 m from the shower core position) for different primaries overlap significantly.

Thus, for the multivariate analysis the key for determination of the elemental composition is the availability of a large number of measured EAS parameters. The feature selection problem is solved by implementing one-dimensional, correlation and multidimensional selection procedures. In figure 4 the three-dimensional plots of EAS parameters are apparently distinct for iron and

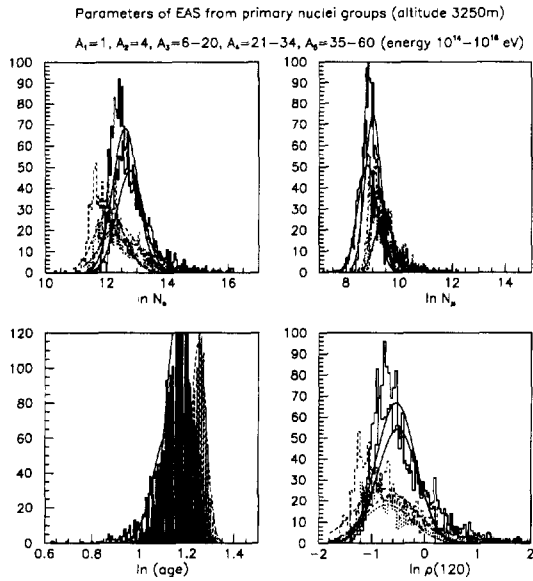


Figure 3. One-dimensional distributions of EAS parameters (see text)

proton showers (altitude 3250 m above sea level).

As one can see from figure 5 adding additional EAS observables increases significantly the accuracy of the energy estimation. The accuracies are different for different nucleus groups and better for heavy nuclei, as expected. The introduction of the detector response (KRETA data, see section 6) deteriorates the accuracies, but the usage of additional parameters (as the number of muons in the central detector N_{μ}^{CD}) can improve the situation.

The comparison of accuracies achievable at mountain and sea level experiments (see figure 6) reflect the obvious fact that shower fluctuations just after reaching the maximum are significantly lower than at the end of development. Recently, for the ANI experiment a new directly measurable parameter (the electron density at a distance of 120 m from the shower axis) has been introduced [17]. that enables the energy estimation independent of the primary. The correlation of this parameter with energy is larger than with number of electrons and muons. The use of this parameter

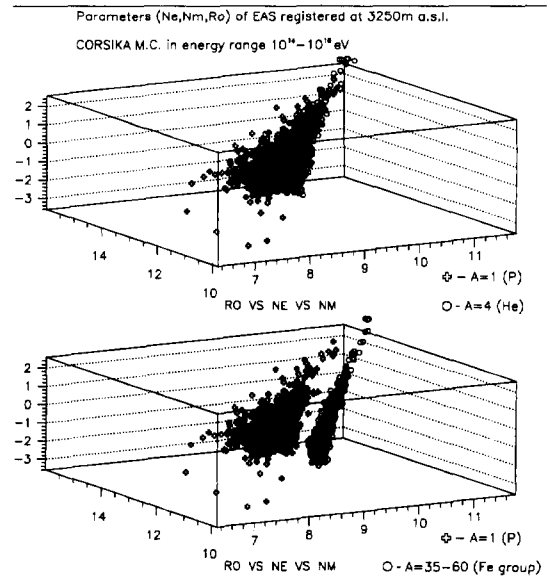


Figure 4. Three-dimensional scatter plots of selected EAS features

with others like age leads to an improved accuracy.

5. Mass discrimination of primaries

As local nonparametric models the Bayesian decision method and regression method were applied to the CORSIKA simulations with and without the detailed simulation of the KASCADE and ANI installations. The local models use the neighborhood (in the multidimensional space of measured EAS parameters) information to decide about the particle and energy type. The Neural Networks are trained on the whole training sample, providing global solutions on the expenses of time consuming, complicated training strategies.

In figure 7 these methods are compared in the task of classifying multidimensional EAS data on the basis of the observables (number of electrons, muons and shower age were used) into the 5 categories, proton, helium, oxygen, silicon and iron. Each of 5 control samples (1000 independ-

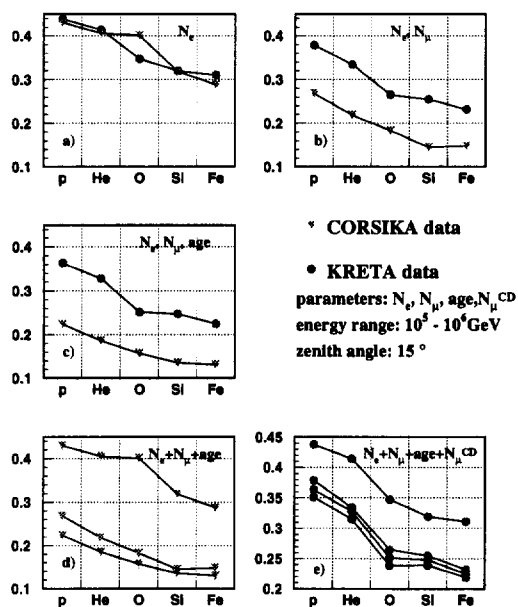


Figure 5. (CORSIKA data: detector response not included; KRETA data: detector response included (see section 6)) Comparison of the accuracy of energy estimation using different sets of observables: a) - c): using successively more observables; d): only CORSIKA data; e) only KRETA data

ent simulation trials) consists of "pure" particles of the mentioned groups and the proportions of their classifications to different nucleus groups are presented.

The results demonstrate rather good consistency of all nonparametric methods, proving relevance and power of the nonparametric methodology. The Bayesian decisions are superior to the regression methods, as in the latter case only one nearest neighbor was used.

In figure 8 the classification probabilities deduced from the mountain altitude and sea level simulations are compared showing clearly the advantages at mountain altitudes. For sea level two modes are presented corresponding to the case of including the "known" primary energy to en-

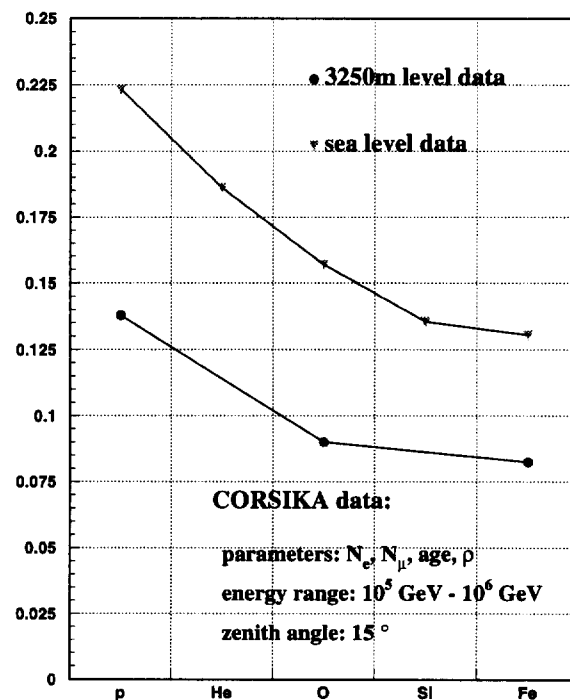


Figure 6. The accuracy of energy estimation at different altitudes using the nonparametric regression method (sea level and 3250 m level data)

able direct comparison with mountain altitudes and the realistic case, when only numbers of electrons and muons have been used for classification.

6. Detector response

The results presented in the previous section concerned the ideal case of knowing exact numbers of electrons and muons in the EAS. To estimate the bias due to finite sampling and reconstruction errors a detailed detector simulation of the KASCADE experiment on the basis of the GEANT package was made taking into account all shower particles, absorbers and active materials, energy deposits, times, trigger conditions and efficiencies, as well as the electronics, digitization of pulse-heights, times, etc...

In the second step the KASCADE reconstruc-

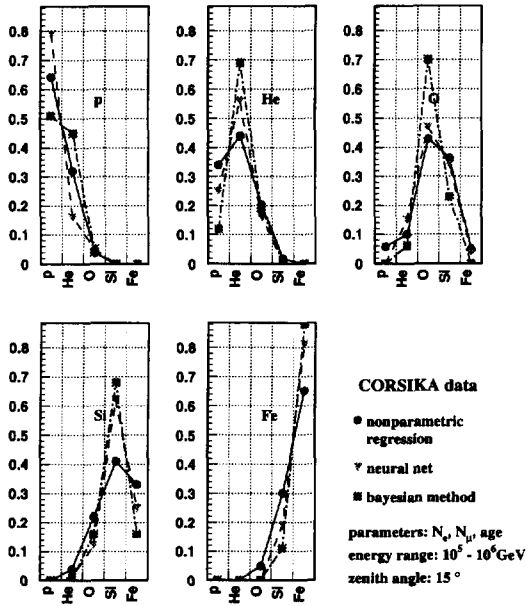


Figure 7. Primary nucleus classification by neural, Bayesian and regression methods (simulated data) (see text)

tion program (KRETA) was applied. The EAS core position, arrival direction, electron- muon densities, electron and muon numbers from the array, hadron information, arrival time distributions in the central detector, and many other characteristics were calculated.

In figure 9 the classifications using pure simulation and including the detector response are compared, as done for the energy estimation in figure 5. As expected, the misclassification rates increase for the realistic experimental situation and resolving protons and alpha particles is very doubtful, but the overall results are satisfactory and the primary identification (especially for proton and iron) still remains reliable.

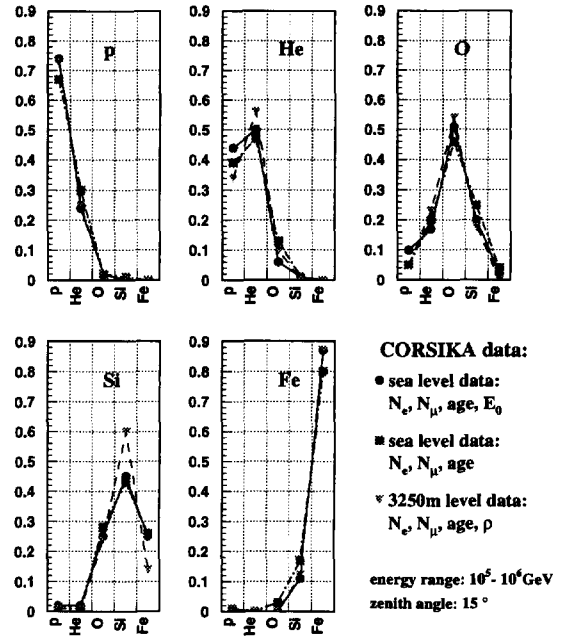


Figure 8. Comparison of primary nucleus classification at different altitudes using the Bayesian method (sea level and 3250m level data)

7. Acknowledgments

This work is part of a scientific cooperation project X131.2 between Forschungszentrum Karlsruhe, Germany and Yerevan Physics Institute, Armenia and was partly supported by the research grant N 94-694 of the Armenian government.

REFERENCES

1. Ichimura M et al., Phys. Rev. D48 (1993) 1949
2. Asakimori K. et al., Proc. 23rd ICRC Calgary, 2 (1993) 21
3. Khristiansen G.B., Kulikov J.V., Solovjova V.I., Pis'ma V., JETP 18 (1958) 353
4. Bierman P.L., Cassinelly J.P., Astron. Astroph. 277 (1993) 691
5. Stanev T. et al., Astron. Astroph. 274 (1993) 902
6. Chilingarian A., Zazyan H., Nuovo Cimento

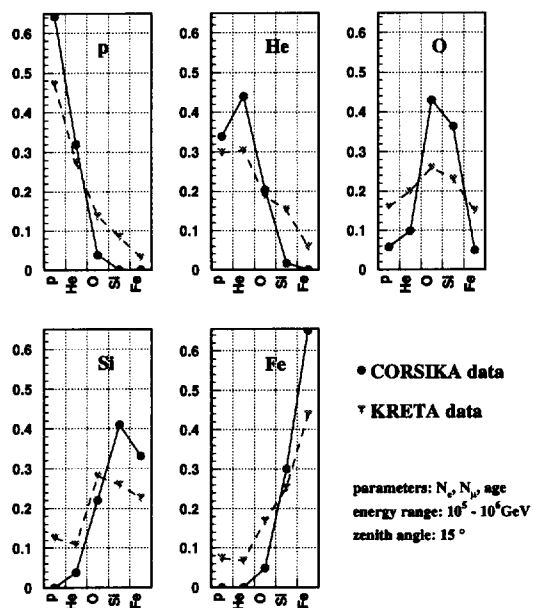


Figure 9. Comparison of primary nucleus classification of simulation data with and without accounting for the detector response (nonparametric regression method)

- 14C (1991) 555
7. Chilingaryan A., Computer Physics Communications 54 (1989) 384
 8. Chilingarian A., Zazyan H., Pattern Recognition Letters 11 (1990) 781
 9. Danilova T.V. et al, Nucl. Instr. and Meth., A323 (1992) 104
 10. H. O. Klages et al. (KASCADE Collaboration), Proc IXth Int. Symp. on Very High Cosmic Ray Interactions, Karlsruhe 1996
 11. Capdevielle J.N. et al., Kernforschungszentrum Karlsruhe, Report KfK 4998 (1992)
 12. Chilingarian A., ANI, Nonparametric Statistical Analysis of High Energy Physics and Astrophysics Experiments, User guide, Version 94.4, unpublished
 13. Aharonyan F., Chilingaryan A. et al., Nucl.

Instr. and Meth., A302 (1991) 522

14. Chilingarian A.A., Pattern Recognition Letters 16, (1995) 333.
15. Chilingarian A.A., Neurocomputing 6, (1994) 497.
16. Ruck D.W., Rogers K.S. et al, IEEE Trans. on Neural Networks 1, (1990) 296
17. Martirosov R., Procureur J., Stamenov J.N., Nuovo Cimento 108A (1995) 299